



A Mode Propagation Database Suitable for Code Validation Utilizing the NASA Glenn Advanced Noise Control Fan and Artificial Sources

Daniel L. Sutliff
Glenn Research Center, Cleveland, Ohio

NASA STI Program . . . in Profile

Since its founding, NASA has been dedicated to the advancement of aeronautics and space science. The NASA Scientific and Technical Information (STI) program plays a key part in helping NASA maintain this important role.

The NASA STI Program operates under the auspices of the Agency Chief Information Officer. It collects, organizes, provides for archiving, and disseminates NASA's STI. The NASA STI program provides access to the NASA Aeronautics and Space Database and its public interface, the NASA Technical Reports Server, thus providing one of the largest collections of aeronautical and space science STI in the world. Results are published in both non-NASA channels and by NASA in the NASA STI Report Series, which includes the following report types:

- **TECHNICAL PUBLICATION.** Reports of completed research or a major significant phase of research that present the results of NASA programs and include extensive data or theoretical analysis. Includes compilations of significant scientific and technical data and information deemed to be of continuing reference value. NASA counterpart of peer-reviewed formal professional papers but has less stringent limitations on manuscript length and extent of graphic presentations.
- **TECHNICAL MEMORANDUM.** Scientific and technical findings that are preliminary or of specialized interest, e.g., quick release reports, working papers, and bibliographies that contain minimal annotation. Does not contain extensive analysis.
- **CONTRACTOR REPORT.** Scientific and technical findings by NASA-sponsored contractors and grantees.

- **CONFERENCE PUBLICATION.** Collected papers from scientific and technical conferences, symposia, seminars, or other meetings sponsored or cosponsored by NASA.
- **SPECIAL PUBLICATION.** Scientific, technical, or historical information from NASA programs, projects, and missions, often concerned with subjects having substantial public interest.
- **TECHNICAL TRANSLATION.** English-language translations of foreign scientific and technical material pertinent to NASA's mission.

Specialized services also include creating custom thesauri, building customized databases, organizing and publishing research results.

For more information about the NASA STI program, see the following:

- Access the NASA STI program home page at <http://www.sti.nasa.gov>
- E-mail your question to help@sti.nasa.gov
- Fax your question to the NASA STI Information Desk at 443-757-5803
- Phone the NASA STI Information Desk at 443-757-5802
- Write to:
STI Information Desk
NASA Center for AeroSpace Information
7115 Standard Drive
Hanover, MD 21076-1320



A Mode Propagation Database Suitable for Code Validation Utilizing the NASA Glenn Advanced Noise Control Fan and Artificial Sources

Daniel L. Sutliff
Glenn Research Center, Cleveland, Ohio

Prepared for
SciTech 2014
sponsored by the American Institute of Aeronautics and Astronautics
National Harbor, Maryland, January 13–17, 2014

National Aeronautics and
Space Administration

Glenn Research Center
Cleveland, Ohio 44135

Acknowledgments

The author would like to acknowledge the efforts of D. Podboy, L. Smith, R. Loew, B. Groening, E. Mysliwicz, and J. Mirecki of TFOME for their support in model assembly and testing. This work was supported by the Fundamental Aeronautics, Subsonic Fixed Wing Project.

Trade names and trademarks are used in this report for identification only. Their usage does not constitute an official endorsement, either expressed or implied, by the National Aeronautics and Space Administration.

This work was sponsored by the Fundamental Aeronautics Program at the NASA Glenn Research Center.

Level of Review: This material has been technically reviewed by technical management.

Available from

NASA Center for Aerospace Information
7115 Standard Drive
Hanover, MD 21076-1320

National Technical Information Service
5301 Shawnee Road
Alexandria, VA 22312

Available electronically at <http://www.sti.nasa.gov>

A Mode Propagation Database Suitable for Code Validation Utilizing the NASA Glenn Advanced Noise Control Fan and Artificial Sources

Daniel L. Sutliff
National Aeronautics and Space Administration
Glenn Research Center
Cleveland, Ohio 44135

Abstract

The NASA Glenn Research Center's Advanced Noise Control Fan (ANCF) was developed in the early 1990s to provide a convenient test bed to measure and understand fan-generated acoustics, duct propagation, and radiation to the farfield. A series of tests were performed primarily for the use of code validation and tool validation. Rotating Rake mode measurements were acquired for parametric sets of: (i) mode blockage, (ii) liner insertion loss, (iii) short ducts, and (iv) mode reflection.

1.0 Introduction

The NASA Glenn Research Center (GRC) has been involved in several programs (Advanced Subsonic Technology, Quiet Aircraft Technology, and the Fundamental Aeronautics Subsonic Fixed Wing) whose goals were the reduction in transport aircraft noise attributed to the turbofan engine. A component of turbofan noise (Ref. 1) is the fan noise caused by rotor-stator, and other interactions, coupled to duct propagation that radiates to the farfield. Computational aero-acoustic (CAA) codes and unique measurement tools are required to enable the development of noise reduction technologies. In order to validate these codes and tools, it is necessary to have an acoustic database.

Parametric studies were performed for several conceptual representations: (i) mode blockage due to stator vanes or rotor blades, (ii) liner insertion loss, (iii) the effects of short ducts on radiation, and (iv) mode reflection due to duct terminations. The intent is not to document specific cases as relevant to a modern turbofan but to provide a database for code validation. Nor will a significant portion of the data be presented, but rather limited samples. The database was acquired on the Advanced Noise Control Fan (Refs. 2 and 3) (ANCF) test bed that was built in the early 1990s (Refs. 4 and 5) to evaluate noise reduction concepts and to provide databases for CAA code validation. Figure 1 shows the Aero-Acoustic Propulsion Laboratory where the ANCF is located and Figure 2 is a photo of the ANCF.

A Configurable Fan Artificial Noise System (CFANS) was utilized to generate and control circumferential modes (m). The system consists of four axially distributed rows, each with 16 circumferentially distributed sets of electromagnetic drivers flush mounted on the inner wall. There are two spool pieces, each having two driver rows (see Figure 3). A LabVIEW (National Instruments Corporation) program is used to generate the waveforms sent to each driver independently, in the proper phase relationship to generate the desired circumferential mode. The signals to each row can be adjusted globally to effect the radial distribution, if desired. The practical limits of the system are $|m\text{-order}| \leq 7$, and frequency ≤ 1500 Hz. Figure 4 shows the typical high quality output from the CFANS for a sample case where mode $m = 2$ was the target mode generated. The upper row of 3-D "tombstone" plots is at 480 Hz (equivalent to BPF on ANCF) and the lower row is for 960 Hz (equivalent to 2BPF). The two columns represent data from two different builds (limited teardown and reassembly, about one month apart) for a limited repeatability demonstration. The target mode is at least 20 dB above any other individual mode, and mostly 10 dB above the sum of all other extraneous modes. This is shown in the small bar graph above and to the right of the 3-D plot. The repeatability (admittedly limited) is within a decibel. Table I provides the modes generated and their cut-off ratios for several hub-to-tip ratios

(σ) inside the duct, for the studies documented in this paper. The modes were measured by the Rotating Rake mode measurement system mounted at the duct radiation plane. The Rotating Rake (Ref. 6) system was developed and implemented by GRC in the 1990s to measure turbofan duct acoustic modes. The system is a continuously rotating radial microphone rake that is inserted into the duct. It provides a complete map of the acoustic duct modes present in a ducted fan. The schematics call out the location of the rotating rake measurement location(s), generally at the duct inlet or exit planes. Figure 5 shows the propagation angles that are referenced in the relevant sections.



Figure 1.—Aero-Acoustic Propulsion Laboratory



Figure 2.—Advanced Noise Control Fan

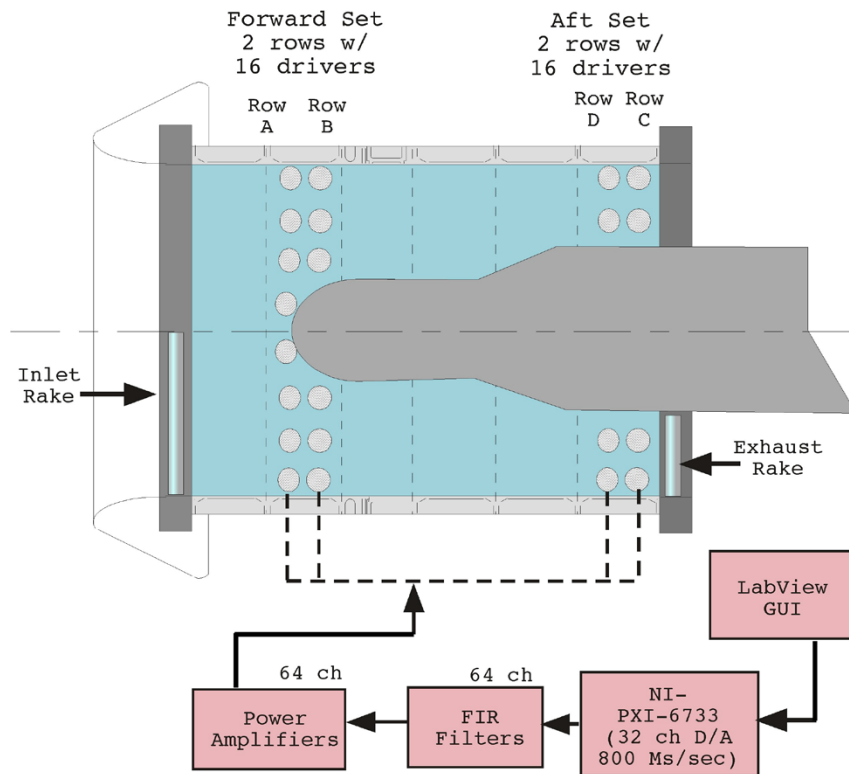
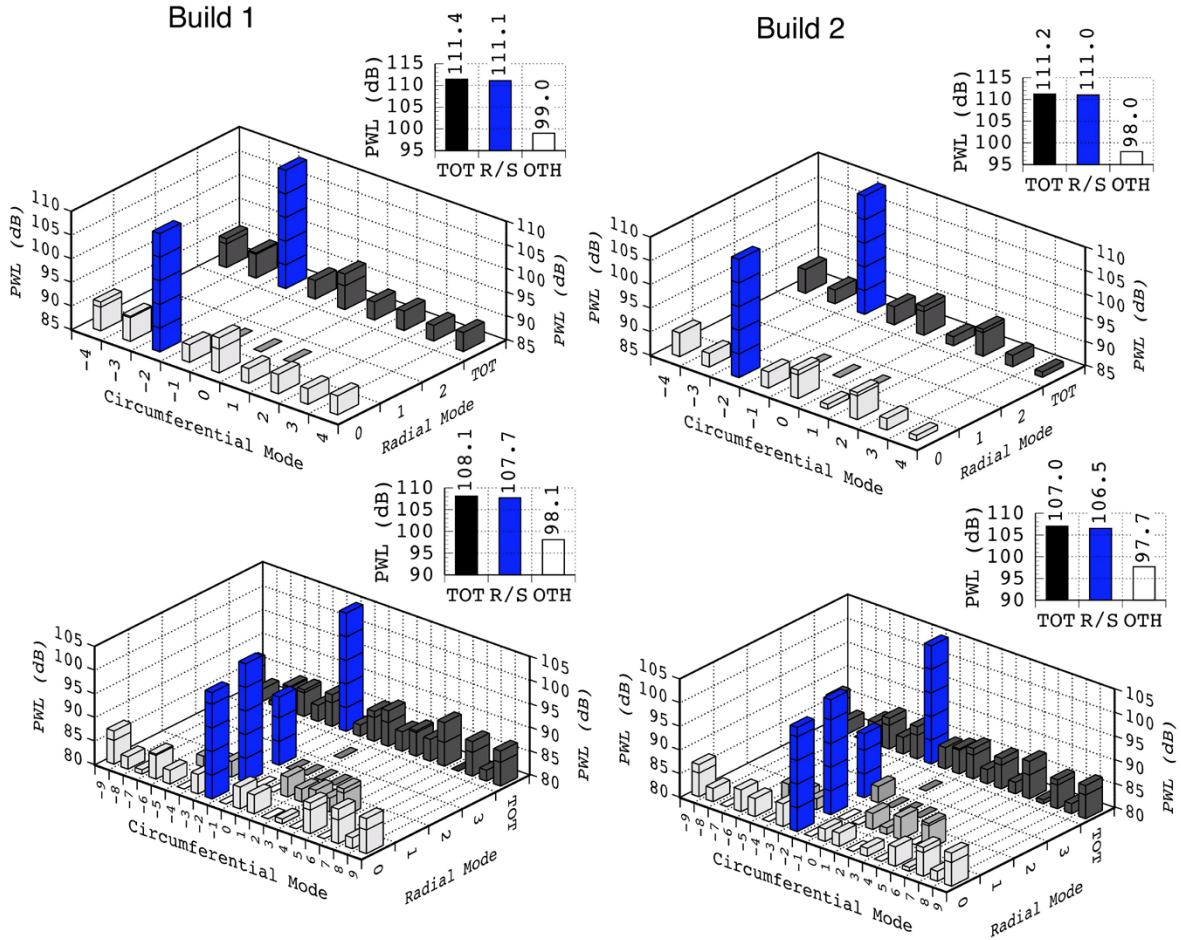


Figure 3.—Schematic of Configurable Fan Artificial Noise System

480Hz * Mode 2

960Hz * Mode 2



TOT—Total Power in Harmonic (all modes)
R/S—Power in Rotor/Stator Interaction Mode
OTH—Power in other modes (non-R/S modes)

Figure 4.—Sample Output of Configurable Fan Artificial Noise System

TABLE I.—MODES GENERATED FOR PARAMETRIC STUDIES USING CFANS

Frequency (Hz)	Modes	Cut-off ratios (σ , hub-to-tip ratio)		
		Inlet ($\sigma = 0.0$)	R/S ($\sigma = 0.375$)	Exhaust ($\sigma = 0.5$)
480	$\pm(2,0)$	1.77	1.89	2.01
	$\pm(4,0)$	1.02	1.03	1.04
580	$+(2,0)$	2.14		
600	$+(2,0)/(2,1)$	2.21/1.01		
700	$+(2,0)/(2,1)$	2.58/1.17		
880	$+(2,0)/(2,1)/(2,2)$	3.24/1.48/0.99		
960	$\pm(2,0)/(2,1)/(2,2)$	3.54/1.61/1.08	3.79/1.72/1.02	4.03/1.53/-
“ ”	$\pm(4,0)/(4,1)$	2.03/1.16	2.06/1.22	2.09/1.22
“ ”	$\pm(6,0)$	1.44	1.45	1.45

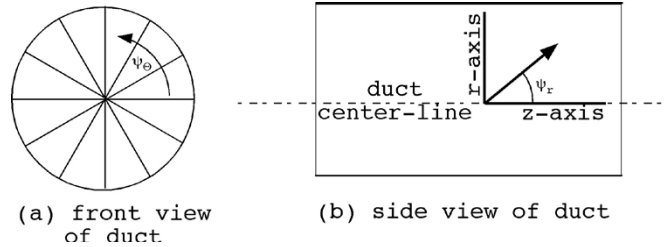


Figure 5.—Schematic of ANCF in Blockage Configurations

2.0 Mode Blockage

2.1 Setup

The objective of this portion of the test was to obtain the effect of geometrical obstructions on mode propagation, i.e., blockage (or transmission loss). Blockage effects were measured separately for stationary geometry (stator vanes) or for rotating geometry (fan blades). In order to provide a larger database, and taking advantage of the flexibility inherent in a no-flow condition, the existing ANCF stator vanes were pitched at a range of angles. Geometry of fixed 3-D surfaces prevented pitching the stator vanes a full 90° , therefore the tip gap was increased to allow for this rotation. The center-body was retained, creating a transition from $\sigma = 0$ at the inlet to $\sigma = 0.5$ at the exhaust exit plane. These configurations are shown schematically in Figure 6 and pictorially in Figure 7.

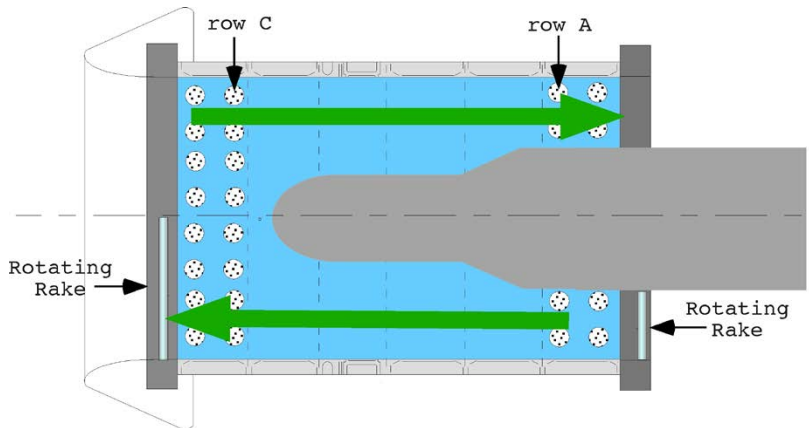
The baseline case was a clean duct, with no stator vanes or fan blades. A parametric set of modes (Table I) were generated at either the forward or aft driver set, and measured by the opposite rotating rake. That is: modes generated by the forward driver set were measured by the exhaust rake; modes generated by the aft driver set were measured by the inlet rake. Fourteen or 28 stator vanes were installed at various pitch angles (Table II) and the rake mode measurements repeated. Separately, the rotor blades were installed at three different pitch angles. The nominal pitch angle for ANCF is 28° and that configuration was run at three different fan speeds. The fan pitch angle was changed by $\pm 10^\circ$ and run at a single fan speed for those two angles.

The assumption is made that the source does not change so that the blockage can be computed by subtracting the mode PWL measured with stators installed from the mode PWL measured in the clean configuration (either with flow or without flow). The configurations were tested over a period of several weeks whereby the ambient temperature varied by 10°F . The mode frequencies generated were at constant frequency, corrected to standard day (59°F). Note that this is standard for duct propagation, but does not take into account any changes in the driver response due to changes in actual driver frequency.

2.2 Results

The blockage is defined as the mode amplitude measured by the rotating rake with the duct in the clean configuration minus the mode amplitude measured with the desired blockage installed between the source and the rake. Thus, a positive number indicates the mode amplitude has been reduced due to blockage.

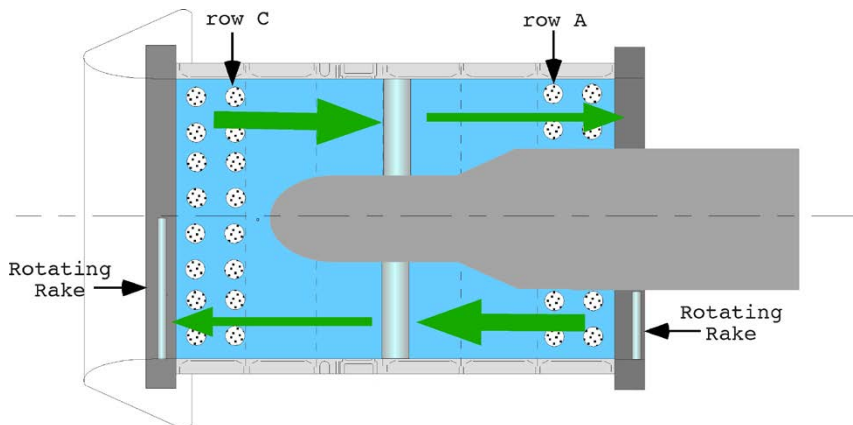
Figure 8 shows the results for mode blockage at various stator vane configurations for modes at 480 and 960 Hz. The blockage for the forward propagating direction (generated by the aft drivers, propagation through the obstruction, and measured by the inlet rake) is shown in Figure 8(a) (480 Hz) and Figure 8(b) (960 Hz).



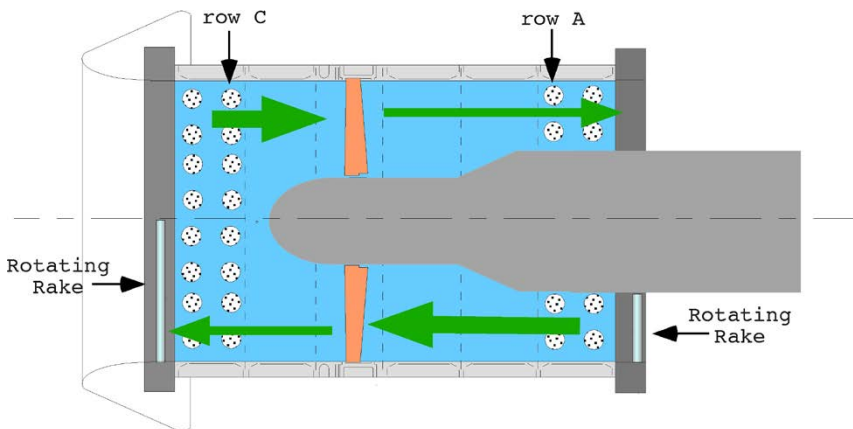
(a) Clean Duct

Modes generated by driver spools are measured at opposite rake.

Assumption is source does not change with the insertion of blockage or the addition of flow.



(b) Stationary Blockage



(c) Rotating Blockage

Figure 6.—Schematic of ANCF in Blockage Configurations

TABLE II.—BLOCKAGE CONFIGURATIONS TESTED

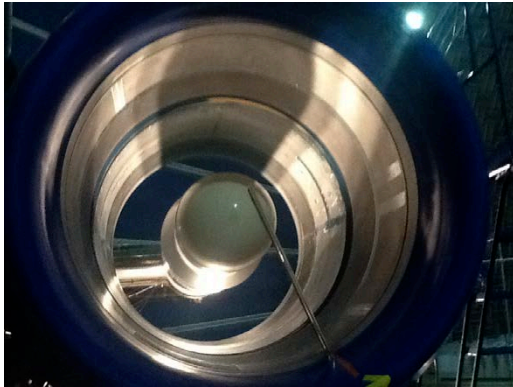
(a) Stator vane configurations

14 vanes	28 vanes
-----	$\alpha=20^\circ$
$\alpha=45^\circ$	$\alpha=45^\circ$
$\alpha = 45^\circ \sim \delta = 1.63 \text{ in.}$	$\alpha = 45^\circ \sim \delta = 1.63 \text{ in.}$
$\alpha = 90^\circ \sim \delta = 1.63 \text{ in.}$	-----

Designation: Pitch Angle (α) ~ tip gap (δ)

(b) Fan blade configurations

$\theta = 18^\circ (1800 \Omega)$
$\theta = 28^\circ (0, 900, 1800 \Omega)$
$\theta = 38^\circ (900 \Omega)$



(a) Clean Duct Configuration



(b) 28 Vane—45° Pitch Configuration

Figure 7.—Photos of ANCF in Mode Blockage Configurations

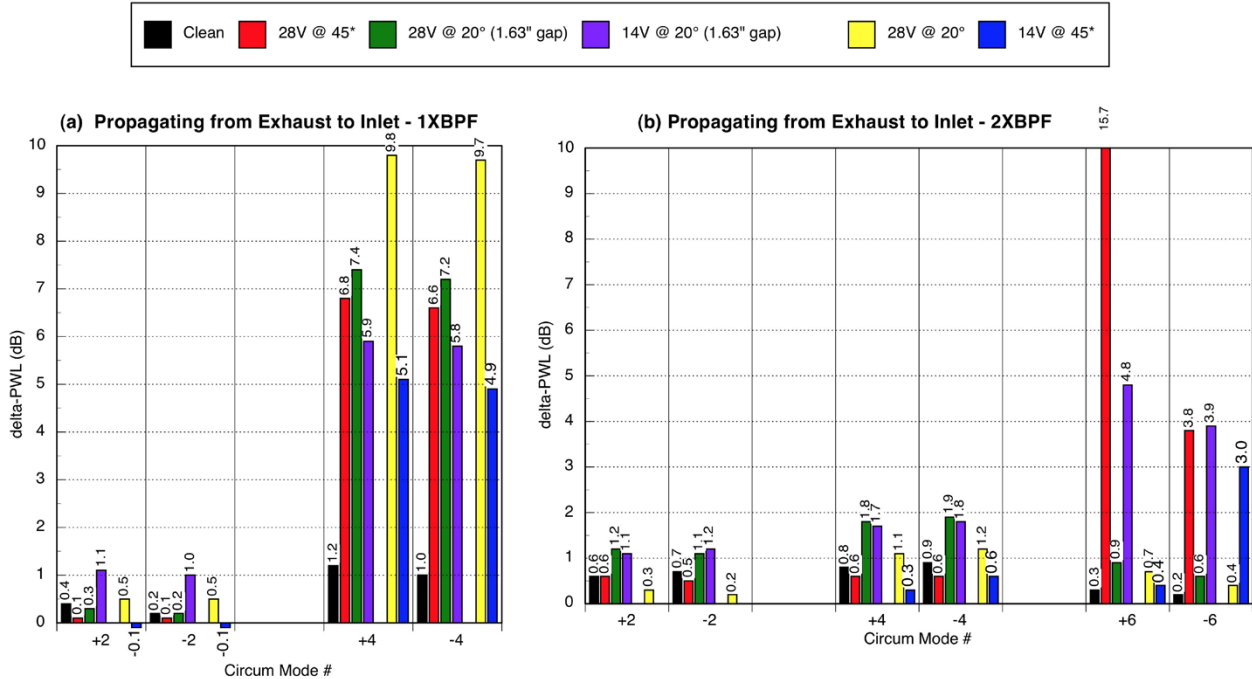


Figure 8.—Circumferential Mode Blockage Levels from Stator Vanes

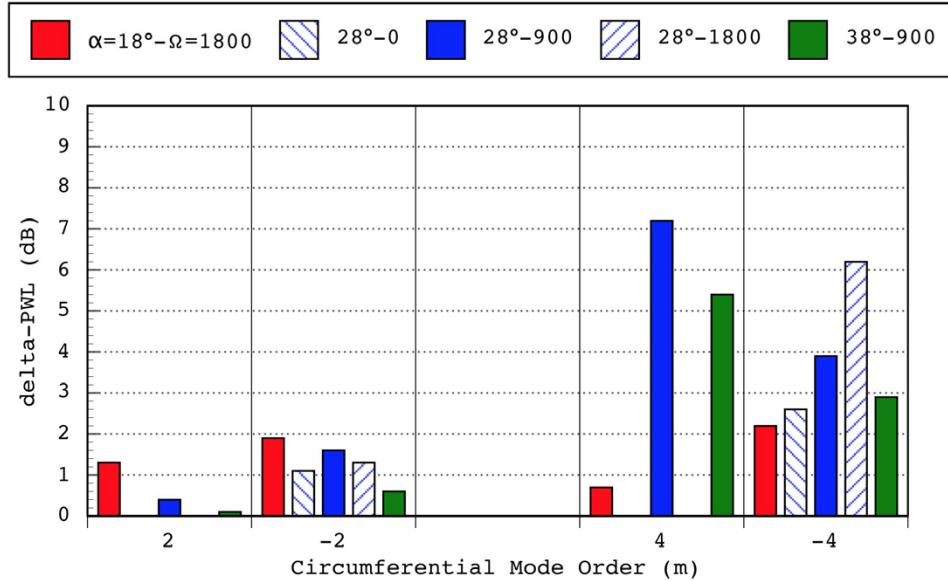


Figure 9.—Circumferential Mode Blockage Levels from Rotor Vanes

The case labeled clean is actually the difference between two clean cases several weeks apart. As such it can provide an estimate of the significance for a measured blockage value. This number is about ± 1 dB. Anything less than that cannot be assumed to be a result relevant to blockage.

Little blockage is seen at low m -orders in either direction. These modes' circumferential propagation angles are relatively low as a result of their higher cut-off ratio. The higher order circumferential modes (four at 480 Hz, six at 960 Hz) are significantly blocked as a result of their higher circumferential propagation angles (Ψ_0)—see Figure 5(a). The stator vane count is seen to increase the mode blockage levels. Thus, it appears as if projected area is the biggest influence on blockage levels under these conditions.

Blockage levels obtained with the rotor (alone) at various rotor RPM (Ω) and pitch angles (α) are shown in Figure 9.

3.0 Liner Evaluation

3.1 Set-Up

Figure 10 shows the schematic of the ANCF configuration for the evaluation of insertion loss due to a liner. The liner used was a single-degree-of-freedom (SDOF) liner with a screen mesh on a 34 percent-open-area (POA). The normalized design resistance for the liner is $1.7\rho c$. The liner core depth is 0.85 in.; resonance frequency is 3221 Hz.

The rotating rake ring was installed in one of two locations: upstream (Figure 10(a)) of the liner to measure the modal PWL at the entrance, and downstream (Figure 10(b)) of the liner to measure the modal PWL at the liner exit. Comparing the two results in liner insertion loss (positive number indicates attenuation). These rake configurations were tested for both the liner exposed and taped over (to provide a hard-wall baseline).

3.2 Results

Figure 11 shows the mode PWLs measured at the entrance and the exit for the hard-wall and the liner. Figure 11(a) shows that at BPF the insertion loss is minor—not surprising as this frequency was not the

design frequency. Note that in general the comparison of the mode strength at the entrance to the HW is comparable to the mode strength at the entrance of the liner. An exception is that mode 4 HW to SW entrance comparison shows a huge variation in PWL. This is thought to be due to being close to cut-off and being more susceptible to reflections. Figure 11(b) shows the insertion loss at 960 Hz, near the target design of the liner. The attenuation is much greater, and increases as the mode number increases. This is expected as the higher mode numbers have lower cut-off ratios—it is generally accepted that liners are more effective at cut-off ratios near unity (Ref. 7) since the mode angle is propagating into the liner (see Figure 5(b)).

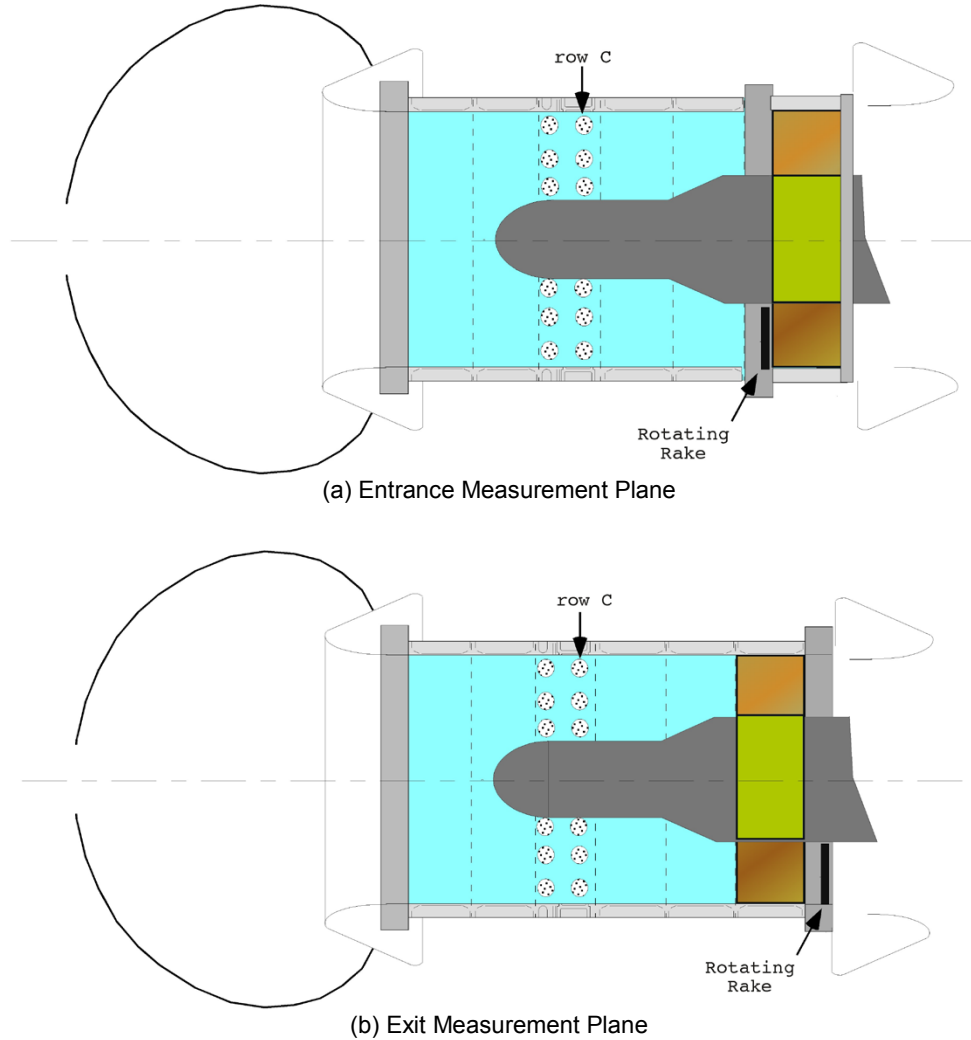


Figure 10.—Schematic of Liner Configurations Tested

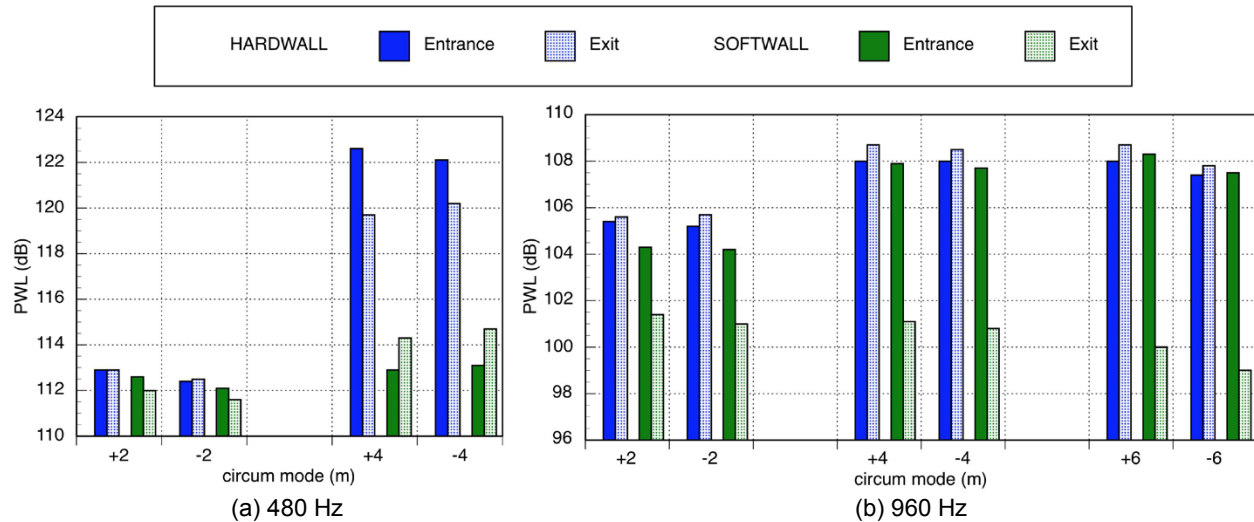


Figure 11.—Liner Configurations Results

4.0 Short-Duct Effects

Duct mode propagation theory assumes a long duct as defined by the Length to Diameter ratio ($L/D > 1$) in order for the classic mode structure to develop along the predicted analytical forms. In reality, even a cut-off mode can be said to “propagate” from the source, albeit at a significant decay rate. Modes that are well below cut-on may decay at a rate of 80 to 100 dB per duct diameter, while a mode just below cut-on may decay at a rate of only 2 to 3 dB per diameter (Ref. 8).

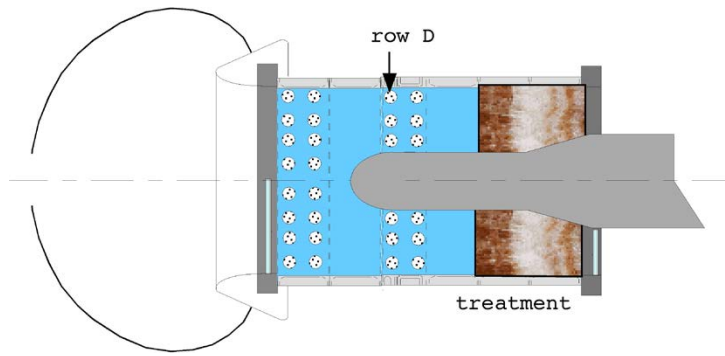
4.1 Set-Up

To investigate this effect, the ANCF/CFANS was tested in two duct lengths, with the actuated driver row 1 diameter from the duct exit, and 1/4-diameter from the duct exit (Figure 12). The modes were measured at the inlet entrance plane. The duct exit was filled with absorptive material to prevent reflections as well as farfield contamination from duct aft radiation. For this portion of the test, corresponding far-field directivity data were acquired. The farfield array was kept at a constant distance from duct inlet entrance plane.

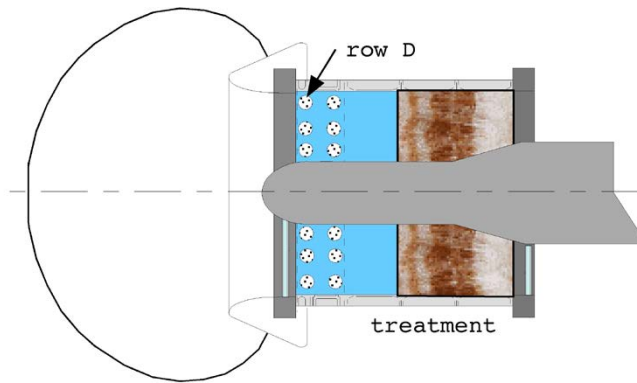
4.2 Results

Typical in-duct mode results for the two duct lengths are shown in Figure 13. The generated mode was $m = +2$ or $m = -2$. Figure 13(a) shows the modal decomposition. For the long duct all of the “extraneous” modes have decayed to the measurement floor ~ 75 to 80 dB. The modes in the short duct configuration have not decayed, nearly equal in strength to the target mode. Figure 13(b) illustrates this by comparing the total PWL in all modes, PWL in the generated mode, and the sum of the non-target mode. For the long duct the majority of the power is in the target mode, for the short duct the extraneous modes carry more energy.

The effect in the far-field indicates that the modes measured at the inlet plane do in fact propagate to the farfield. Figure 14 shows the tonal directivity for $m = \pm 2$. The long duct directivity shows the characteristic flat lobe associated with a well cut-on mode. Note the symmetry between the positive and negative mode. The pattern radiated from the short duct shows significant departure from the classical directivity. It also shows an asymmetry between the positive and negative generated mode. These effects are due to axisymmetric variation (Ref. 9) resulting from multiple modes.



(a) Long Duct, $L/D = 1$



(b) Short Duct, $L/D = 1/4$

Figure 12.—Effect of Duct Length on In-Duct Modes

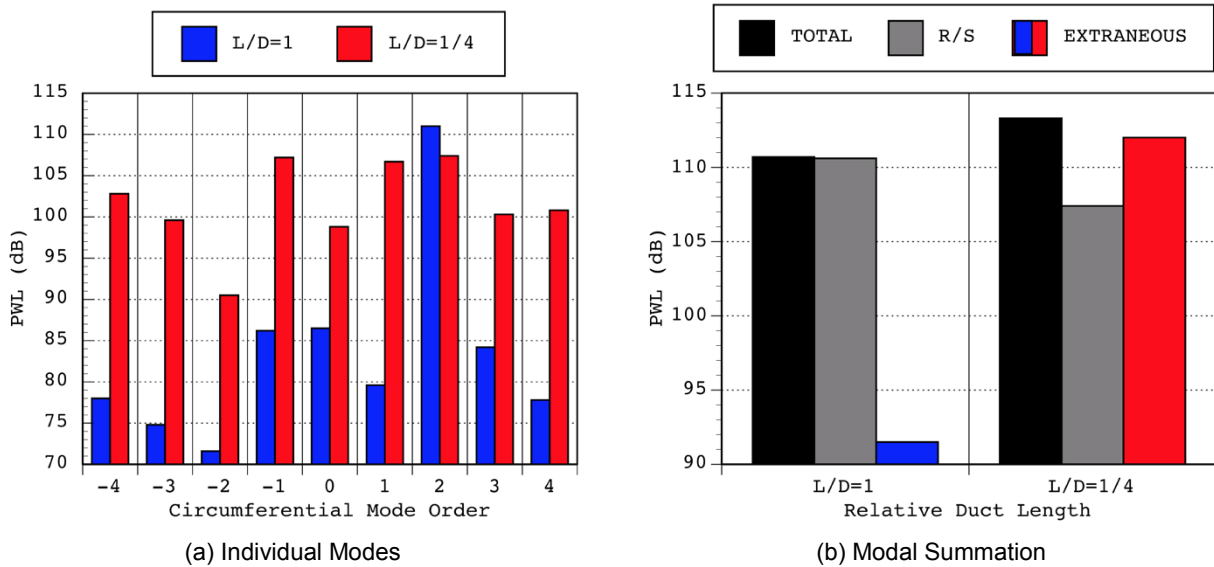


Figure 13.—Effect of Duct Length on In-Duct Modes

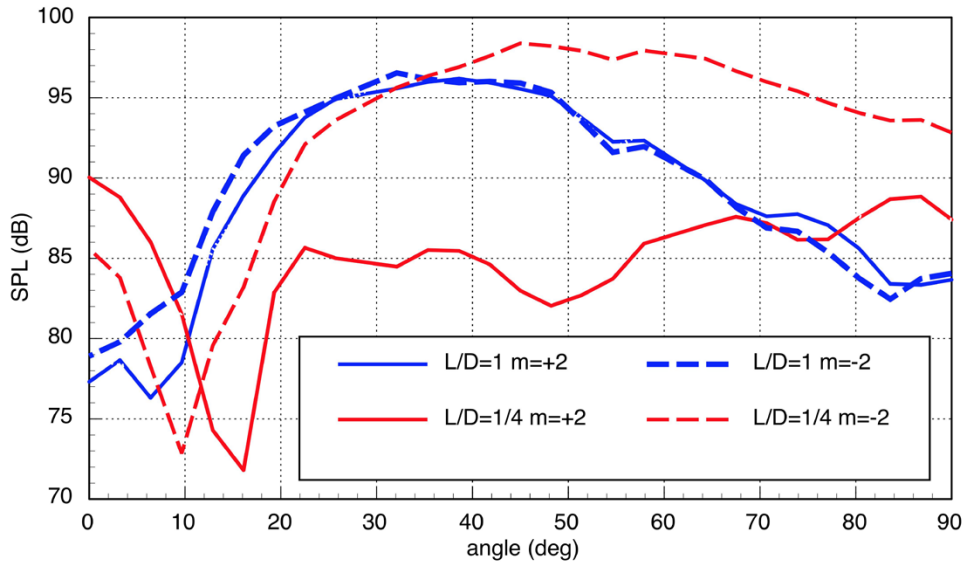


Figure 14.—Effect of Duct Length on Far-field Directivity

5.0 Mode Reflection

5.1 Setup

In order to provide a clean, cylindrical duct, for this experiment the ANCF was built up off of the stanchion that normally supports the fan and duct sections that make up the nacelle. That is, the spool pieces were stacked up in a vertical orientation based on the floor. This removed center-body and support pylon from the arrangement, providing a constant area cylindrical duct. Two configurations were tested in this setup: (a) with the flow lip attached, and (b) without the flow lip attached, which left a bare flange as the exit termination (Figure 15 and Figure 16). The entire stack rested on the floor, and approximately 6 in. of foam material was placed in the bottom of the stack to minimize reflections from the floor.

Typically, a single rake, extending from the outer-wall to the duct centerline, has been mounted to measure duct modes. It has been known (Refs. 10 and 11) that measuring at a single axial location will not be able to account for reflections in the duct, therefore, for this experiment an additional rake was mounted on the same rotating ring as the original. This second rake was adjustable in the axial direction over the range of 2.5- to 10.5-in., in fixed, 1-in. increments, and was mounted 180° in the circumferential direction from the original rake, which remains fixed in the axial direction. Figure 17(a) and Figure 17(b) show this arrangement.

Data were acquired from the dual rakes in order to provide the two-point axial variation needed to compute the reflection. Reflections were created using two methods. The first method relies on the natural reflections due to an open-ended exit termination. The ring containing the dual rotating rake system was mounted at the exit of the ANCF stack-up (Figure 15(a)). The single driver row (C) farthest from the exit termination was used to generate the modes in Table I. This configuration was run with the flow lip attached—this was assumed to minimize reflections, and with the flow lip removed, creating a sharp 90° flanged exit—this was assumed to create reflections. A second configuration was used to generate artificial reflections, see Figure 15(b). This was accomplished by locating the dual rake ring in the center of the stack-up. Driver row C was used to generate the “primary” wave and driver set B was used to generate the “reflected” wave. Each driver row was actuated independently and the modes were measured by the dual rakes. Then both sets were activated simultaneously and the resulting superposition was measured.

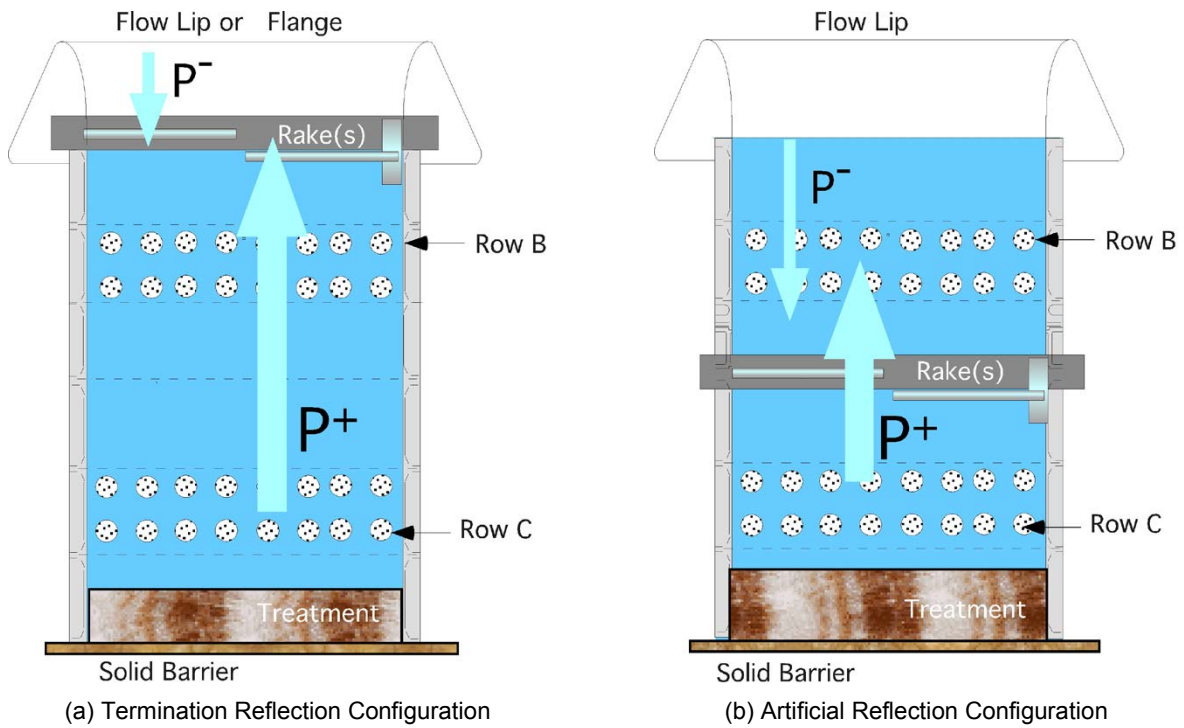


Figure 15.—ANCF in Mode Reflection Configurations

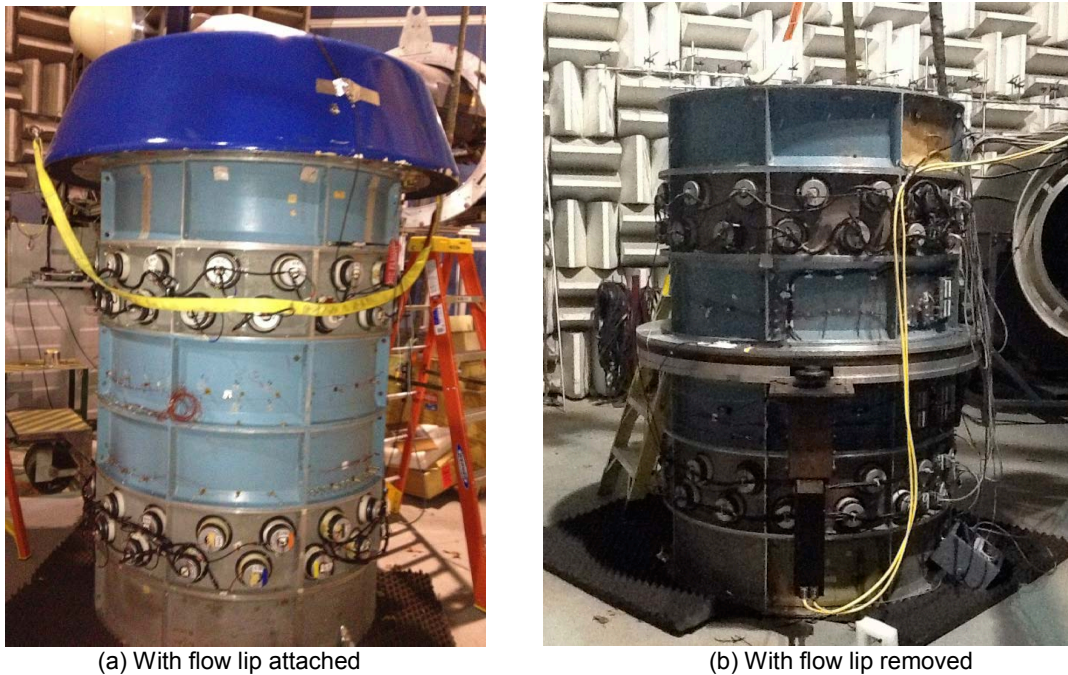


Figure 16.—ANCF in Off-Stanchion Configuration

The concept is that the measured combination $\overline{B + C}$ is the resulting superimposed mode and is equal to $B+C$ measured independently and mathematically combined. Thus any technique to separate the “primary” from the “reflected” wave will result in B and C that can be compared to the independent measurements for code validation (B and C are arbitrary amplitudes generated by driver rows B and C).

